American Mineralogist, Volume 69, pages 928–936, 1984

Cation arrangement in iron–zinc–chromium spinel oxides

CLARE P. MARSHALL AND WAYNE A. DOLLASE

Department of Earth and Space Sciences
University of California
Los Angeles, California 90024

Abstract

The distribution of ferric and ferrous ions within the quaternary Fe^{2+}–Fe^{3+}–Zn–Cr spinel solid solution series is documented using Mössbauer spectroscopy and X-ray diffraction. Along the binary joins $FeCr_2O_4$–Fe_3O_4, $ZnCr_2O_4$–Fe_3O_4 and $ZnFe_2O_4$–Fe_3O_4 the cation distribution changes from normal to inverse. From the different trends of iron distribution versus composition observed along these three joins and at other points within the Fe–Zn–Cr solid solution series, it was found that octahedral site ferric/ferrous charge hopping may be the most important phenomenon stabilizing the inverse ion distribution. For spinels whose compositions make charge hopping impossible or statistically unlikely, cation distribution is governed by the intrinsic spinel site preferences (tetrahedral site: Zn > Fe^{2+} Fe^{3+} >> Cr, octahedral site: Cr > Fe^{3+} > Fe^{2+} > Zn), which result from the size and bonding characteristics of these atoms.

Near the $ZnFe_2O_4$–Fe_3O_4 edge of this spinel quadrilateral, the normal to inverse transition proceeds essentially to the maximum extent allowed by the Zn content, because the octahedral Fe^{2+} produced by inversion can share electrons with the surrounding octahedral Fe^{3+} ions. Inversion along the $FeCr_2O_4$–Fe_3O_4 edge of the quadrilateral, however, is inhibited until there is a sufficient octahedral Fe^{3+} population to make electron sharing (with inversion produced octahedral Fe^{2+}) statistically likely. A rapid change of site preference of iron ions occurs in the central range of this composition subspace, offering a physical reason for the miscibility gap found along the chromite–magnetite join.

Introduction

Cation arrangement in spinel-type oxides has long been a topic of interest among mineralogists (Barth and Posnjak, 1932; Verwey and Heilmann, 1947; Robbins et al., 1971; Price et al., 1982), because the site distribution (particularly of iron) has a strong effect on magnetic, electrical and thermochemical properties. Studies of a variety of end member spinel compositions (Verwey and Heilmann, 1947, Navrotsky and Kleppa, 1967; Price et al., 1982; Urusov, 1983; O'Neill and Navrotsky, 1983) and binary solid solutions (Olés 1970; Dobson et al. 1970; Levenstein et al. 1972; Grandjean and Gérard 1978, and Burns 1981, to mention a few) have brought into focus many problems concerning the compositional dependance of cation distribution in spinels. This paper will concentrate on changes in cation arrangement within a quaternary solid solution series, the Zn–Cr–Fe^{2+}–Fe^{3+} spinel oxide system.

The spinel structure consists of an almost cubic close packed array of oxygen atoms with cations in intersticies within the oxygen framework. Sixteen octahedral and eight tetrahedral sites within one unit cell of 32 oxygens are filled, in the system studied, with zinc in the tetrahedral sites, chromium in the octahedral sites and ferric and ferrous iron in either site. The octahedra form edge sharing chains along [110]. The tetrahedra are isolated from one another, sharing each of their corners with three octahedra.

Chromite ($FeCr_2O_4$), $ZnCr_2O_4$ and franklinite ($ZnFe_2O_4$) are all normal spinels, with divalent atoms on the tetrahedral sites. Magnetite ($FeFe_2O_4$) is an inverse spinel with all of its ferrous iron occupying the octahedral site. (The degree of inversion, which in these spinels is equal to the fraction of tetrahedral site occupied by trivalent ions, is commonly denoted by λ which can vary from 0 to 1.) Thus, this system exemplifies the transition from one end member ordering state to the other, across a quaternary solid solution series. By using Zn and Cr, which strongly prefer tetrahedral and octahedral sites respectively (Navrotsky and Kleppa, 1967), the only distributional variables are the position and valence of the iron atoms present. These constraints allow the cation distribution vs. composition of the experimentally produced phases to be found using X-ray powder diffraction (XRD) and Mössbauer spectroscopy.

Experimental procedures

Seventeen spinels were synthesized from mechanical mixtures of oxide powders within the Zn–Cr–Fe^{2+}–Fe^{3+}

0003–004X/84/0910–0928$02.00

Table 1. X-ray data for synthesized spinels

no.	# comp, (Zn, Cr) rest=Fe	temp, dur. (°C, hours)	f O2 aprox. values	##unit cell dimension ± 2 σ (Ångstroms)
31	1.0, 2.0 +	1200,3	air	** 8.3275(6)
7	0.90,2.0 +	960,26	-14.5	* 8.3333(7)
6	0.80,2.0 +	1000,24	-14.5	* 8.3375(8)
8	0.55,2.0 +	940,25	-14.5	* 8.3503(11)
10	0.30,2.0 +	940,25	-14.5	* 8.3616(14)
30	1.0,1.60 +	1200,18	air	** 8.3502(8)
28	0.75,1.50	1060,10	-13.2	** 8.3660(11)
29	0.25,1.50	1060,4	-14.0	** 8.3938(10)
15	1.0, 1.0 +	850,24	air	** 8.3826(9)
21	0.50,1.0	1007,48	-13.1	** 8.3904(6)
33	1.0,0.55 +	1200,3	air	** 8.4099(24)
26	0.75,0.50	985,3	-10.0	** 8.3965(6)
38	0.25,0.50	1010,11	-13.0	** 8.3869(10)
25	0.05,0.50	985,3	-13.0	** 8.3864(6)
32	1.0, 0.0 +	1200,3	air	** 8.4415(12)
34	0.75, 0.0	912,10	-12.1	** 8.4366(6)
36	0.50, 0.0	1025,4	-12.0	** 8.4252(11)

\# assuming complete conversion of the starting mix
Cu K α_1 = 1.540598, Cu K α_2 = 1.54443
\+ synthesized with a Li-borate flux
* NBS silicon standard used
** Silver metal used as standard

spinel quadrilateral, except along the magnetite–chromite join, amply studied by Robbins et al., (1970); Levinstein et al., (1972); Ok et al., (1978); and others (compositions on Figure 2 and Table 1). One spinel was synthesized near the magnetite–chromite join (sample 25). It showed characteristics consistent with the findings of these authors. Most samples were pressed, then hung from platinum wire in a controlled atmosphere gas mixing furnace (CO–CO_2) operated between 900°C and 1100°C.

All samples were quenched by dropping, under an argon atmosphere. The samples reached room temperature within minutes, although the exact quench rate was not measured. If wüstite or hematite was found in the X-ray pattern, or if the diffraction pattern showed broad peaks, the samples were reground and rerun at slightly changed oxygen fugacities until no other phases could be detected. Final conditions are included in Table 1. The compositions listed in Tables 1 and 2 are those assuming complete conversion of the starting mixes to spinel. Mössbauer and X-ray data were consistent with this assumption (to within 4% of the expected composition) except for sample 26. For that single sample, both the X-ray and Mössbauer measurements are more consistent with a composition of Zn 0.70, Cr 0.56, rather than the originally intended composition, Zn 0.75, Cr 0.50. The corrected composition is shown in Figures 2 and 3.

Mössbauer spectra were collected on a conventional constant acceleration spectrometer with a moving ^{57}Co in Pd source and powdered sample absorbers. The mirror image spectra, accumulated on a 512 channel multichannel analyser, employed velocity increments of about 0.03 mm/sec/channel for paramagnetic spectra and about 0.08 mm/sec/channel for magnetic spectra. The samples were placed in 1-inch diameter polyethelene holders with inert adhesive. Velocity calibration utilized Fe metal and Na-nitroprusside.

Room temperature Mössbauer spectra were collected for each spinel synthesized, (see Table 2). In paramagnetic spectra, doublets were constrained to have equal areas and peak widths. In magnetic spectra, the areas for each sextet were constrained to a 3:2:1 ratio, with corresponding peaks constrained to have equal peak widths. (For a more detailed description of the experimental procedures, see Marshall, 1983.)

The calculated and measured cation arrangement of these spinels is assumed to correspond to the temperature of synthesis because the quench rates were rapid relative to ionic re-equilibration rates of similar spinels (Trestman-Matts et al., 1983). The electronic configurations of the iron atoms, however, probably does not quench (O'Neill and Navrotsky, 1984; Trestman-Mattes et al., 1983) and could represent lower temperatures, although the cation arrangements predicted by Robbins et al., (1971) along the chromite–magnetite join correspond to the theoretical thermodynamic arrangement (O'Neill and Navrotsky, 1984) predicted for 1000°C, the synthesis temperature.

Experimental results

The parameters obtained from the Mössbauer spectra are isomer shift (IS), quadrupole splitting (QS) and peak

Table 2. Mössbauer data for synthesized spinels[$]

No.	#comp (Zn, Cr rest=Fe	##IS (mm/ sec)	QS (mm/ sec)	PW (mm/ sec)	H kOe (±5)	rel. area	λ Möss. meas. ±0.06	λ UCE calc. ±0.02
31	1.0,2.0	-	-	-	0	-	-	0.0
7	0.90,2.0	0.88(2)	0.17	0.30(1)	0	1.0	0.0	0.0
6	0.80,2.0	0.88(1)	0.21	0.30(1)	0	0.89(1)	0.0	0.0
		0.34(9)	0.28	0.30(1)	0	0.11(1)		
8	0.55,2.0	0.85(1)	0.26	0.376(5)	0	1.0	0.0	0.0
10	0.30,2.0	0.90(1)	0.23	0.359(8)	0	1.0	0.0	0.0
30	1.0,1.60	0.364(9)	0.348	0.278(7)	0	1.0	0.0	0.0
28	0.75,1.50	0.968(9)	0.284	0.397(8)	0	0.343(1)	0.0	0.03
		0.403(15)	0.408	0.286(9)	0	0.657(1)		
29	0.25,1.50	0.96(1)	0.33	0.403(9)	0	0.605(1)	0.0	0.01
		0.38(1)	0.43	0.383(6)	0	0.395(1)		
15	1.0,1.00	0.339(8)	0.385	0.322(4)	0	1.0	0.0	0.0
21	0.50,1.00	?	?	?	?	?	?	0.20
33	1.0, 0.55	0.351(4)	0.345	0.33(3)	0	1.0	0.0	0.0
26	0.75,0.5*	0.28(9)	-0.02	0.73(3)	468	0.18(2)	0.30*	0.25
		0.61(7)	0.09	2.14(3)	413	0.82(2)		
38	0.25,0.50	0.21(5)	0.03	0.57(2)	507	0.32(1)	0.71	0.68
		0.65(5)	0.06	1.45(5)	449	0.69(1)		
25	0.05,0.50	0.26(6)	0.10	0.55(1)	497	0.33(1)	0.81	0.77
		0.67(5)	0.11	1.36(2)	445	0.67(1)		
32	1.0, 0.0	0.331(4)	0.414	0.343(5)	0	1.0	0.0	0.0
34	0.75,0.0	?	?	?	?	?	?	0.18
36	0.50,0.0	0.20(8)	0.06	0.74(4)	499	0.11(1)	0.31	0.43
		0.53(13)	0.02	2.34(4)	440	0.89(1)		

$ measured at room temperature, source was Co in Pd.
\# assuming complete conversion of the starting mix to spinel
rel to Fe. (errors are the same for QS)
* Composition would be 0.70,0.56 (rather than 0.75,0.50) if the Mössbauer peak areas are correct.
** assuming excess ferrous iron on the octahedral site is charge hopping
? value was not obtained.

width at half height (PW). The IS is approximately constant for a particular iron valence state in a particular type of site. A literature search of oxide spinels gives the following averages relative to iron metal: tetrahedral Fe^{2+} = 0.91 mm/sec (9 examples), octahedral Fe^{2+} = 1.02 mm/sec (8 examples), tetrahedral Fe^{3+} = 0.28 mm/sec (6 examples) and octahedral Fe^{3+} = 0.37 mm/sec (14 examples). QS is a function of the electric field gradient and therefore measures the symmetry of the site. In oxide spinels, QS for either tetrahedral or octahedral Fe^{3+} tends to be small (0.3–0.6 mm/sec) and relatively insensitive to cation disorder. On the other hand, Fe^{2+} in octahedral and especially tetrahedral sites show small to very large QS values, depending upon disorder of near neighbor sites. The PW reflects the similarity of the sites within each crystal; for a spinel where all of the tetrahedral ferrous ions have an identical configuration of nearest neighbors, the peak width will be narrow (around 0.3 mm/sec.). Broader peaks result from the existence of dissimilar sites, differing, for example, by having different second or third nearest neighbors.

The room temperature Mössbauer spectra of all paramagnetic samples showed spinels with "normal" distribution ($\lambda = 0.0$), i.e., in these samples, all ferric iron is in octahedral coordination and all ferrous iron is in tetrahedral coordination.

Samples along the $ZnCr_2O_4$–$ZnFe_2O_4$ binary join showed IS, QS and PW consistent with octahedral ferric iron as was found also by Muthukumarasamy et al., (1980). Samples along the $ZnCr_2O_4$–$FeCr_2O_4$ binary join show typical tetrahedral ferrous iron values of IS, QS and PW. Along this join the QS remains almost constant and is very small (0.18 to 0.26 mm/sec.). This is expected because, along this join the local site symmetry is high with all of the nearest neighbor cations for this site being the same (Cr atoms). The small changes in QS are probably due to variations among the second nearest neighbor cations, i.e., the Fe and Zn on the tetrahedral site. The largest QS on this join occurs at an approximately half and half mixture of zinc and iron on the tetrahedral site, where the highest degree of disorder would occur.

Mössbauer spectra of samples 28 ($Zn_{0.75}Fe_{0.75}Cr_{1.50}O_4$) and 29 ($Zn_{0.25}Fe_{1.25}Cr_{1.50}O_4$) show contributions from both octahedral ferric and tetrahedral ferrous iron. The values of QS of the ferric iron are close to those obtained along the $ZnCr_2O_4$–$ZnFe_2O_4$ join. The QS for the ferrous iron, however, is higher than values obtained along the $ZnCr_2O_4$–$FeCr_2O_4$ join, as a result of decreased local site symmetry caused by mixing of different ion species on the nearest neighbor octahedral site. The width of both the ferric and ferrous Mössbauer peaks are broader than the average width measured along the simpler binary joins. According to the site distribution calculations utilizing unit cell edge, (next section) these two samples also contain minor amounts of tetrahedral ferric and octahedral $Fe^{2.5+}$, (i.e., they are partially inverse) which could also contribute to the peak broadening.

The magnetic spectra showed spinels which were either partially or fully inverse ($0.3 < \lambda < 1$, see Table 2). These spectra are much more complicated and overlapped than the paramagnetic spectra and the errors in measurement are consequently larger.

In general the magnetic spectra looked similar to those of Robbins et al. (1971). In every magnetic spectrum, one sextet had an IS value correspnding to tetrahedral Fe^{3+} (around 0.27 mm/sec). For these, QS is close to 0.0 as would be expected from the high symmetry of the site. The peak width averaged around 0.7 mm/sec, which is wider than ideal.

The octahedral site sextet in the magnetic spectra is more complicated. Whenever both ferric and ferrous iron are present on the octahedral site, an intermediate IS value of about 0.63 mm/sec was observed, corresponding to an intermediate valence state resulting from electron charge hopping between ferric and ferrous ions (Bauminger et al., 1961; Dobson et al. 1970; Robbins et al. 1971; Murray and Linnett, 1976; Ok and Evans, 1976; Lotgering and van Diepen, 1977 and Ok et al., 1978). The quadrupole interaction of this sextet varies between 0.06 to 0.25 mm/sec. The peaks are broad, around 1.4 mm/sec for samples with approximately equal numbers of ferric and ferrous ions, and up to 2.3 mm/sec when greatly different proportions of ferric and ferrous ions occupy the octahedral site. These extremely wide peaks are attributable to variable amounts of charge transfer between iron ions, depending on the ion distribution around each site.

Although a minor tetrahedral Fe^{2+} component is present in some of the magnetic spectrum samples, its spectral contribution is too weak to show a third discernable sextet. Lack of resolution of this sextet no doubt contributes to the apparent broadened peakwidths of the two fitted sextets.

Several room temperature spectra in the central range of this composition space showed both paramagnetic and magnetic contributions of varying proportions. The paramagnetic component is due to the interaction of smaller magnetic domains within the samples, i.e. superparamagnetism (Greenwood and Gibb, 1971, p. 104).

The presence of both paramagnetic and magnetic components yield severely overlapped, low resolution spectra. Sample 34 ($Zn_{0.75}Fe_{2.25}O_4$) shows a largely paramagnetic spectrum with enough magnetic component to produce an undulating background, similar to that observed by Topsoe et al. (1974, Fig. 2-B). Sample 21 ($Zn_{0.50}Fe_{1.50}Cr_{1.0}O_4$) consists of about half paramagnetic and half magnetic components at room temperature, yielding a series of broad humps spanning the entire velocity range, similar to Figure 2, Grandjean and Gerard (1978). Although the paramagnetic component decreased when the temperature was lowered (also seen by Topsoe et al. 1974), individual peaks were still difficult to resolve.

Site distribution calculations

Mössbauer parameters

Using the chemical compositions of the starting mix and the relative peak areas of the Mössbauer spectra, site

distributions for each of the synthetic spinels were calculated. The calculation is straightforward for paramagnetic spectra, where the ferric iron is confined to octahedral sites and the ferrous iron is in tetrahedral sites. The assumptions involved are: all Zn is in tetrahedral coordination, all Cr is in octahedral coordination and all the sites of the spinel structure are full.

For the magnetic spectra, only the tetrahedral ferric iron to total iron area ratio was used for the calculation. The Mössbauer peaks corresponding to the tetrahedral site are narrower and better resolved than those corresponding to the octahedral peaks.

From the calculated site occupancy, the inversion parameter λ is found (i.e., the amount of tetrahedral ferric iron, see Table 2, λ Möss. meas.). The estimated error in the inversion parameter is ±0.06 when errors in fit and relative areas on the Mössbauer spectra are taken into account.

Cell dimensions

Distinguishing between tetrahedral and octahedral ions using Mössbauer spectroscopy alone is somewhat imprecise, especially when magnetic or mixed magnetic and paramagnetic spectra are involved. Furthermore, changes in site occupancy that involve less than 5% of the total iron are not generally distinguishable by Mössbauer measurements. For these reasons, estimations of site occupancies were also made using unit cell edge measurements.

Interatomic distances (such as the tetrahedral atom–oxygen bond length and octahedral atom–oxygen bond length) can be calculated from a knowledge of the spinel cell dimension, a, and the single variable positional parameter in the spinel structure, u. (The oxygen atom lies on a 3-fold axis and has fractional coordinates (u,u,u).) Conversely, the values of a and u can be calculated from a knowledge of the t–o (tetrahedral atom–oxygen) and m–o (octahedral atom–oxygen) bond lengths. The operative equations are:

$$a_{calc} = \frac{2\,d_{m-o}^2 - d_{t-o}^2}{\sqrt{\frac{25}{48}d_{t-o}^2 + \frac{11}{16}(d_{m-o}^2 - d_{t-o}^2)} - \frac{5}{\sqrt{48}}(d_{t-o})} \quad (1)$$

$$u_{calc} = \frac{d_{t-o}}{\sqrt{3}\,a_{calc}} + \frac{1}{8} \quad (2)$$

where

d_{m-o} = average octahedral atom–oxygen distances for that composition.

d_{t-o} = average tetahedral atom–oxygen distances for that composition.

a calc. = calculated unit cell edge,

u calc. = calculated oxygen atom fractional coordinate.

Related equations were derived to predict u and from this in turn, a, for end member composition spinels by Hill et al., (1979). (These were also used by O'Neill and Navrotsky (1983) to calculate best fit cation radii for spinel oxides.)

Thus, given a spinel composition and an appropriate set of characteristic cation–oxygen bond lengths, the site occupancy can be varied until the calculated cell dimension matches the observed cell dimension. In considering the possible site distributions, it was assumed that where Zn is present, it is in tetrahedral coordination and where Cr is present, it is in octahedral coordination. Where both ferric and ferrous iron are present on the octahedral site, it is assumed that equal numbers of Fe^{2+} and Fe^{3+} are involved in charge hopping, i.e., the extra electron is shared between two octahedral sites creating a net charge of 2.5. The remaining iron, either Fe^{3+} or Fe^{2+}, is not participating in charge hopping.

This latter assumption is probably not strictly correct as ratios other than 1:1 are possible, as shown by Ok and Evans, (1976), Evans and Ok, (1977), and Ok et al., (1978), but it was initially employed to simplify the calculations. Ignoring charge-hopping on the octahedral site altogether yield calculated unit cell edge dimensions that were much larger than measured values. Calculations made with octahedral Zn or tetrahedral Cr also yielded spurious results.

The values used for characteristic cation–oxygen distances must be chosen carefully. They should not be very different from those measured in other natural crystalline oxides (as given, for example, by Shannon 1976, or Brown and Wu, 1976). They must also be chosen so that the difference between calculated and measured unit cell dimensions of the end members are less than the error in measurement (0.001Å).

For tetrahedral ferric and octahedral $Fe^{+2.5}$, measured cation–oxygen distances from end member magnetite (Fleet, 1981) were used. The other values were chosen to fit the measured unit cell edge dimensions for the other end members of this spinel quadrilateral and, where known, their measured single variable positional parameters, u. Unfortunately, this is an underconstrained system of equations (because the u parameters are not well known) so the values chosen here are not unique. That is, other values of cation–oxygen distances within 0.02Å of those chosen will fit the end members just as well, as long as the difference between Fe^{2+} and Zn t-o distance is 0.035Å and the difference between Cr and Fe^{3+} m-o distance is 0.041Å. Calculated cation–oxygen distances for spinels by O'Neill and Navotsky (1983) do not completely satisfy these constraints. The difference in their Cr and Fe^{3+}–O distance is 0.030Å and their tetrahedral Fe^{+} oxygen distance is 1.865Å rather than 1.888Å as measured by Fleet (1981).

It is important that the cation–oxygen distances be fit to

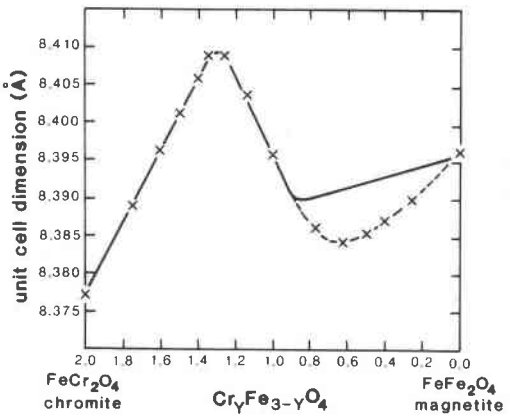

Fig. 1. Unit cell edge as a function of composition along the chromite–magnetite join. X's are measured values from Levinstein et al. (1972). Solid line is calculated using equation (1) assuming charge hopping only among equal numbers of Fe^{2+} and Fe^{3+}. Dashed line is calculated using the assumption that all the octahedral iron atoms are charge hopping.

the end members, because a change in 0.0007Å in the tetrahedral atom–oxygen distance or 0.004Å in the octahedral atom–oxygen distance changes the calculated unit cell dimension by 0.001Å, which is the typical error in measurement. Also, because of the strong site preferences of chromium and zinc, it can be assumed for the end members that a negligible amount of iron ion site exchange has occurred. For tetrahedral sites the values used are (in Ångstroms): Fe^{2+} 2.015, Fe^{3+} 1.888 and Zn 1.980. The octahedral values are: Fe^{2+} 2.154, Fe^{3+} 2.026, $Fe^{2.5+}$ 2.059 and Cr 1.985.

From the calculated site occupancies, the inversion parameter λ is found (i.e., the amount of tetrahedral ferric iron), see Table 2 (λ UCE calc.) and Figure 3. The estimated error for this calculation is ±0.02 when errors in unit cell dimension and cation–oxygen distances are both taken into account. For a complete tabulation of these calculations, see Marshall, 1983.

Discussion

Before considering the general quaternary system, it is useful to first review the binary joins. The $ZnCr_2O_4$–$FeCr_2O_4$ join shows simple substitution of one ion for another on the tetrahedral site, as can be verified by the Mössbauer measurements. The simple substitution results in linear changes in unit cell edge with composition. The $ZnFe_2O_4$–$ZnCr_2O_4$ join similarly shows simple substitution on the octahedral site. Measured unit cell dimensions of this study are in agreement with those of Olés' (1970). Measured Mössbauer parameters are consistent with those of Muthukumarasamy et al. (1980). The calculated site occupancies using unit cell dimensions are also consistent with simple substitution along both of these binary joins.

The $FeCr_2O_4$–Fe_3O_4 join (chromite–magnetite), has been well studied. Francombe (1957) and Levinstein et al. (1972) found extraordinarily nonlinear changes in unit cell dimension with composition. Robbins et al. (1971) and Petric and Jacob (1982) presented predicted site distribution along this binary join, on the basis of Mössbauer spectra and magnetite activity measurements respectively. Ok et al., (1978) predicted site occupancies for the magnetite-rich end members.

Calculated unit cell dimensions (equation 1) utilizing predicted site occupancies of Robbins et al. follow the general trend for changes in unit cell with composition (within 0.01Å) as measured by Francombe (1957) and Levinstein et al. (1972) (see Fig. 1). The predicted site occupancies of Petric and Jacob (1982), however, show trends in calculated unit cell edge very different than those measured. This discrepancy could be due in part to the difference in experimental conditions (1100°C for Robbins et al. vs. 1400°C for Petric and Jacob), but the fact that Petric and Jacob neglected to take into account charge hopping on the octahedral site is also a factor.

In the present study, the "best fit" estimates of site occupancies along the magnetite chromite join are only slightly different from the predictions made by Robbins et al. (1971). For the composition range $Cr_{0.8}Fe_{2.2}O_4$–$FeCr_2O_4$ (see Fig. 1), some ferric iron substitution into the tetrahedral site was necessary to produce a good fit (±0.0005Å) between calculated and measured unit cell dimension. For the composition range Fe_3O_4–$Cr_{0.8}Fe_{2.2}O_4$, the calculated values using Robbins et al.'s predictions and the initial assumptions in this study are larger than the measured values by up to 0.007Å, well beyond measurement error.

The discrepancy is a result of assuming that charge hopping only involves equal numbers of Fe^{2+} and Fe^{3+}. Whenever both Fe^{2+} and Fe^{3+} ions are present on the octahedral site at appropriate hopping temperatures and in sub-equal amounts, the "extra" electrons are shared among all adjacent iron atoms, not only on a 1:1 basis. A similar conclusion has been reached for magnetite-like spinels by other authors (Adler, 1968; Goodenough, 1967; Dobson 1970; Evans and Ok, 1977; Wu and Mason, 1981; Trestman-Matts et al. 1984). To test this hypothesis, the unit cell dimension was recalculated assuming that all the octahedral iron atoms participate in charge hopping (i.e., the electrons form a conduction band on the octahedral site), and that the cation–oxygen distance for the charge hopping species is the same as measured in magnetite (Fleet et al., 1981) where the ratio is 1:1. This assumption produced a very good fit (±0.0005Å) throughout the compositional join (see Fig. 1, dotted curve). The cation distribution near the magnetite end member is essentially identical to the predictions of Ok et al. (1978).

The $ZnFe_2O_4$–Fe_3O_4 join (franklinite–magnetite) has also been well studied (Popov et al., 1963; Dobson et al., 1970; Ok and Evans 1976; Srivastava et al., 1976; Evans and Ok, 1977), though no one study included both XRD and Mössbauer work across the entire join, and the

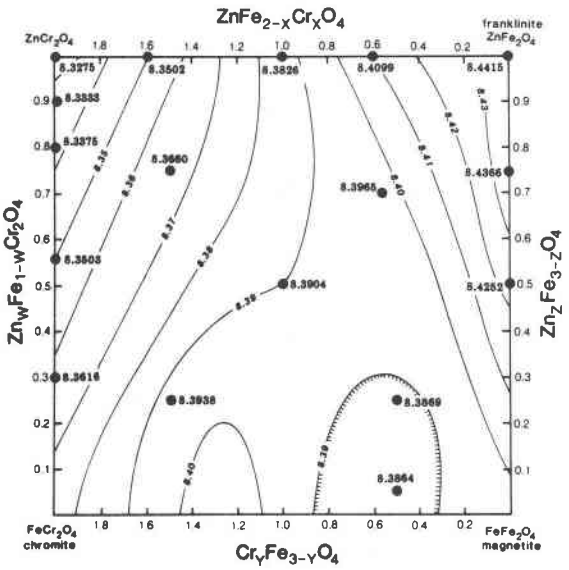

Fig. 2. Unit cell edge contours (interval of 0.01Å) over the Fe^{2+}–Fe^{3+}–Zn–Cr spinel composition space. Boldface numbers are data points from this study. Data for the $ZnFe_2O_4$–$FeFe_2O_4$ join are from Popov et al. (1963) and data for the $FeCr_2O_4$–$FeFe_2O_4$ join are Levinstein et al. (1972).

Dobson and Srivastava studies are not completely consistent. For these reasons, three spinels were synthesized along this join, at 50%, 75%, and 100% franklinite mole proportion.

Unit cell edge measurements of these samples and those of Ok and Evans (1976) are consistent with those made by Popov et al. except for a constant of 0.004Å (Popov et al.'s data are consistently 0.004Å larger than this study's data and other published data on the end members). The unit cell edge vs. composition relation is not as sigmoidal as found on the chromite–magnetite join but does show a change in slope at 70 mole % franklinite, which has been correlated with a change in entropy by Popov et al, (1963).

The Mössbauer measurements of the present study along this join are consisent with those of Dobson et al. (1970). Franklinite shows a paramagnetic spectrum at room temperature. Between $Zn_{0.75}Fe_{2.25}O_4$ and $Zn_{0.60}Fe_{2.4}O_4$, spectra with paramagnetic and ferrimagnetic components are observed, with the paramagnetic component decreasing with decreasing Zn component. For samples less zinc rich than $Zn_{0.60}Fe_{2.4}O_4$, the spectra are entirely magnetic with all of the octahedral ions participating in charge transfer (as in Ok and Evans, 1976). Srivastava et al. (1976) found mixed spectra at 80 mole % franklinite and attributed the paramagnetic component to interactions of small magnetic domains in the crystals.

The tetrahedral site occupancy (calculated from cell dimensions and measured by Mössbauer spectroscopy) along this join between Fe_3O_4 and $Zn_{0.75}Fe_{2.25}O_4$ shows almost complete substitution of ferric iron for Zn. Between $Zn_{0.75}Fe_{2.25}O_4$ and $ZnFe_2O_4$, both ferric and ferrous ions substitute for Zn, with the larger proportion being ferrous (probably because of its more comparable size to Zn ions).

In Figure 2, contours of unit cell edge over the entire composition space studied are presented, incorporating data from this study and from Levinstein et al. (1972) and Popov et al. (1963) for the magnetite–chromite and magnetite–franklinite joins respectively. Although Not all contours in Figure 2 are equally well constrained by the data, this particular configuration of contours is presented because it is most consistent with the site occupancy to be discussed below. The changes in unit cell edge in this composition space are due not only to changes in composition, but also reflect changes in site preference of the iron atoms, as the normal to inverse transition takes place.

It is also interesting to note that on each of the normal to inverse binary joins in this system, the onset of magnetic ordering at room temperature coincides with an inflection in the unit cell dimension and a sharp increase in the amount of ferric iron substituting on the tetrahedral site (i.e., a sharp increase in λ).

Figure 3 presents contours of the amount of tetrahedral ferric iron (that is, the inversion parameter, λ) throughout the composition space, as calculated using equation 1 and the measured and interpolated unit cell edge dimensions shown in Figure 2. The assumption used was that all

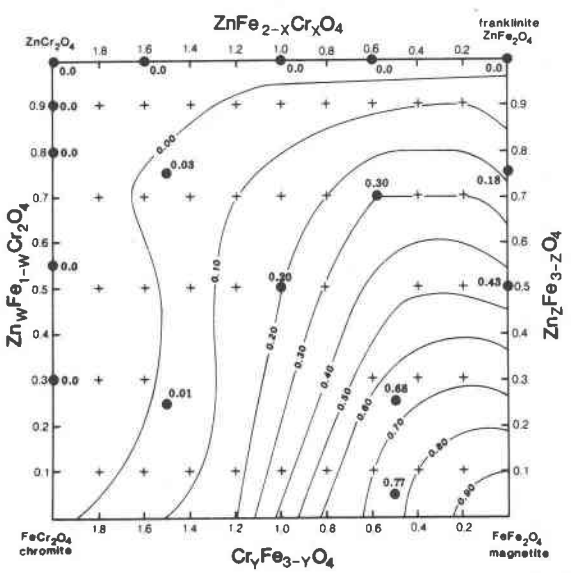

Fig. 3. Contours of the amount of inversion, λ, over the Fe^{2+}–Fe^{3+}–Zn–Cr spinel composition space as calculated using measured unit cell edge dimensions and equation (1) (corresponds identically to amount of tetrahedral ferric iron present). The large dots (●) represent points where the unit cell edge was measured directly. Crosses (+) represent points where unit cell edge values were linearly interpolated between contours on Fig. 2.

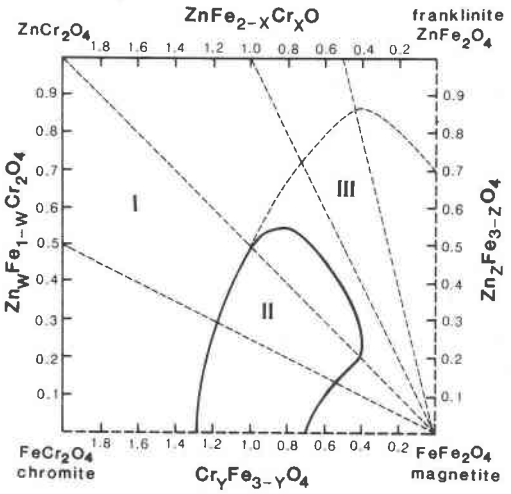

Fig. 4. The rate of change of inversion with composition. Dashed lines are compositional joins along which the rate of change of inversion, $d\lambda/dx$ is measured. Region I, $d\lambda/dx < 1$. Region II, $d\lambda/dx > 1$. Region III, $d\lambda/dx \simeq 1$.

octahedral iron is charge hopping when there is a near 1:1 ratio of ferric to ferrous iron. The cation distribution of any spinel in this composition space (formed near 1000°C), can be determined using Figure 3.

To discuss the degree of inversion as a function of composition, it is useful to divide the composition space into three regions (as was done in Robbins et al., 1971, for the magnetite–chromite join). Although the boundaries between regions are not strictly constrained, Figure 4 shows the general form of the rate of change of inversion with composition, $d\lambda/dx$. The diagram was constructed by drawing compositional joins between points on the $ZnCr_2O_4$–$ZnFe_2O_4$ and $ZnCr_2O_4$–$FeCr_2O_4$ joins and magnetite (see dotted lines, Fig. 4). Along each of these compositional joins, the rate of inversion with composition was calculated. Boundaries separating regions with $d\lambda/dx < 1$, $d\lambda/dx > 1$ and $d\lambda/dx \simeq 1$ were drawn. The error in placement of these boundaries is not more than 10 mole %.

In Region I, both λ and $d\lambda/dx$ are small, that is, very little ferric iron substitutes onto the tetrahedral site. This region can be described in terms of normal spinel site preferences arising from cation size and bonding considerations. In general, for the tetrahedral site, the preferences are: $Zn > Fe^{2+} > Fe^{3+} >> Cr$ and for the octahedral site: $Cr > Fe^{3+} > Fe^{2+} >> Zn$. The difference in tetrahedral site preference beween Fe^{2+} and Fe^{3+} is not very large, as is shown by the presence of small amounts of tetrahedral ferric iron.

In Region II, $d\lambda/dx$ is greater than one. This is a region of high rate of change of inversion with composition signifying a sudden transition from the normal spinel ordering scheme of Region I to the inverse spinel ordering scheme of Region III. Note that this region is not present near the franklinite–magnetite join because the presence of Zn in the tetrahedral site limits the possible degree of inversion.

In Region III, $d\lambda/dx \simeq 1$, that is, the rate of change of inversion is essentially constant with changes in composition. As the composition becomes more magnetite rich in this region, ferrous ions substitute directly onto the octahedral site (ferric ions onto the tetrahedral site) allowing charge hopping among octahedral iron atoms. Charge hopping stabilizes the inverse spinel by raising the entropy (de-localizing electrons) and lowering the strain in the structure (more similar-sized ions on the tetrahedral and octahedral sites). This region can be discussed in terms of a different site preference model than in Region I. That is: tetrahedral $Zn > Fe^{2+} > Fe^{3+} >> Cr$ and octahedral $Cr > Fe^{2.5+} > Fe^{3+} > Fe^{2+} >> Zn$. The energy saved by octahedral charge hopping ($Fe^{2.5+}$) more than compensates for the energy lost by replacing ferrous iron with ferric on the tetrahedral site, and so the inverse arrangement is preferred over the normal cation arrangement at these compositions.

Many factors influence the normal to inverse transition in spinel oxides. In this system, one important feature stabilizing the inverse spinel is the tendency of the iron atoms on the octahedral site to charge hop. This conclusion is similar to that of Robbins et al. (1971) who concluded from the Mössbauer spectra that along the magnetite–chromite join between Fe_3O_4 and $Fe_{1.8}Cr_{1.2}O_4$, the octahedral site maintained equal amounts of ferric and ferrous iron. The main difference between these conclusions is the phrase "equal amounts". As was previously discussed (this study and Ok et al., 1978), a 1:1 correspondence of ferric and ferrous ions is not essential for charge transfer.

Applications

Octahedral site charge hopping is an important stabilizing phenomenon for iron rich inverse spinels, and must be taken into account in thermodynamic models of spinels (or any mineral system with ferric and ferrous ions in adjacent octahedral sites). Of geologic importance are the thermodynamic models using spinels as petrogenetic indicators (Sack, 1982).

In the spinel–olivine geothermometer (Irving, 1965), the partitioning of elements between olivine and spinel is assumed to be dependent only on the temperature of formation and mole fraction of ions on the octahedral site of the spinel. Roeder et al. (1979), however, showed that higher ferric iron spinels yield greater Fe^{2+}/Mg ratios, and that the Fe^{2+}/Mg distribution between ferric rich spinels and olivine is essentially independant of temperature and therefore not useful as a geothermometer. In view of the present study, this observation of Roeder et al. seems not only reasonable but expected, because a ferric rich spinel will incorporate as much ferrous iron in its octahedral sites as possible, to satisfy its charge

hopping capacity. Consequently, the Fe^{2+}/Mg ration will be dependent more on the amount of ferric iron present in the spinel than the temperature of formation.

The change in site preference which results in the normal to inverse cation distribution is probably related to miscibility gaps in reported spinel systems, as shown theoretically by O'Neill and Navrotsky, (1984). One does not find nor would one expect a miscibility gap along the $ZnCr_2O_4$–$ZnFe_2O_4$ or $ZnCr_2O_4$–$FeCr_2O_4$ joins because the compositional changes result in simple substitution of one similar sized cation for another on the octahedral and tetrahedral sites respectively.

Along the franklinite–magnetite join, although a change in site preference does occur, the site substitution rate is still constant with composition. A miscibility gap is not expected until much lower temperatures are reached (O'Neill and Navrotsky, 1984). (This join does not fit their model exactly, however, probably in part because they did not take into account conduction electrons on the octahedral site.) Valentino and Sclar (1982) studied this join at temperatures as low as 500°C, and no miscibility gap was observed. Exsolution lamellae of magnetite in franklinite have been found by Burke and Kieft (1972), but no temperatures were estimated for this occurence.

Along the chromite–magnetite join, a rapid exchange of ferric and ferrous ions occurs (Region II, Fig. 4). Compositions within this region of high rate of site substitution might be expected to exsolve at lower temperatures into a charge hopping species (inverse) and a non-charge hopping species (normal). Cremer (1969) studied the magnetite–chromite join and found a miscibility gap in this region at 900°C, although other studies have placed the miscibility gap as low as 500°C (Evans and Frost, 1975). The miscibility gap has also been calculated thermodynamically by O'Neill and Navrotsky (1984).

Increased pressure should also favor exsolution. As can be seen in Figure 1, the volume of normal and inverse spinels would be substantially smaller than that of the homogenous solid solution. Similarly, Figure 4 shows that the binary join connecting $ZnCr_2O_4$ with magnetite, crosses Region II and, by analogy with the magnetite–chromite join, a miscibility gap in this system is to be expected. No studies have yet been made at low temperatures or high pressures along this join.

Acknowledgments

The authors would like to thank T. O. Mason, A. Navrotsky, H. O'Neill and an anonymous reviewer for useful comments and suggestions in their reviews.

References

Adler, D. (1968) Insulating and metallic states in transition metal oxides. Solid State Physics, 21, 1–113.

Barth, T. F. W. and Posnjak E. (1932) Spinel Structures: with and without variate atom equipoints. Zeitschrift für Kristallographie, 82, 325–341.

Bauminger, R., Cohen, S. G., Marinov, A., Ofer, S. and Segal E. (1961) Study of the low-temperature transition in magnetite and the internal fields acting on iron nuclei in some spinel ferrites, using Mössbauer Absorption. Physical Review, 122, 5, 1447–1450.

Brown, I. D. and Wu, W. K. (1976) Empirical parameters for calculating cation-oxygen bond valences. Acta Crystallographica, B 32, 1957–1959.

Burke, E. A. J. and Kieft, C. (1972) Franklinite from Langban, Sweden, a new occurence. Lithos, 5, 69–72.

Burns, R. G. (1981) Intervalence transitions in mixed valence minerals of iron and titanium. Annual Reviews of Earth and Planetary Sciences, 9, 345–383.

Cremer, V. (1969) Solid solution formation in the Chromite–Magnetite–Hercynite System at 500–1000°C. Neues Jahrbuch für Mineralogie, Abhandlungen, 111, 2, 184–205.

Dobson, D. C., Linnett, J. W. and Rahman, M. M. (1970) Mössbauer studies of the charge transfer process in the system $Zn_{(x)}Fe_{(3-x)}O_4$. Journal of the Physics and Chemistry of Solids, 31, 2727–2733.

Evans, B. W. and Frost B. R. (1975). Chrome-spinel in progressive metamorphism—a preliminary analysis. Geochimica et Cosmochimica Acta, 39, 959–972.

Evans, B. J. and Ok, H. N. (1977) Collective electron states in $Zn_xFe_{3-x}O_4$ and $Cd_xFe_{3-x}O_4$ for $0 < X < 0.3$. Physica 86–88, B + C, 931–933.

Fleet, M. E. (1981) The structure of magnetite. Acta Crystallographica, B37, 917–920.

Francombe, M. H. (1957) Lattice changes in spinel type iron chromites. Journal of the Physics and Chemistry of Solids, 3, 37–43.

Goodenough, J. B. (1967) Narrow band electronics in transition metal oxides. Czechoslovak Journal of Physics, B-17, 304–336. (in English).

Grandjean, F. and Gerard, A. (1978) Observation by Mössbauer Spectroscopy of electron hoppings in the spinel series $Zn_{(1-x)}Ge_{(x)}Fe_2O_4$. Solid State Communications, 25, 679–683.

Greenwood, N. N. and Gibb, T. C. (1971). Mössbauer Spectroscopy. Chapman and Hall, Ltd. publishers.

Hill, R. J., Craigs, J. R. and Gibbs, C. V. (1979) Systematics of the spinel structure type. Physics and Chemistry of Minerals, 4, 317–339.

Irving, T. N. (1965). Chromian spinel as a petrogenetic indicator. Part I, Theory. Canadian Journal of the Earth Sciences, 2, 648–672.

Levinstein, H. J., Robbins, M., and Capio, C. (1972) A crystallographic study of the system $FeCr_2O_4$–$FeFe_2O_4$ $(Fe^{2+}Fe^{3+}_{(x)}Cr_{(2-x)})O_4$. Materials Research Bulletin, 7, 27–34.

Lotgering, F. K. and van Diepen A. M. (1977) Electron exchange between Fe^{2+} and Fe^{3+} ions on octahedral sites in spinels, studied by means of paramagnetic Mössbauer spectra and susceptibility measurements. Journal of the Physics and Chemistry of Solids, 38, 565–572.

Marshall, C. P. (1983) Cation arrangement in Iron–Zinc–Chromium Spinel Oxides. Masters Thesis, University of California, Los Angeles.

Murray, P. J. and Linnett, J. W. (1976) Mössbauer studies in the spinel system $Co_{(x)}Fe_{(3-x)}O_4$. Journal of the Physics and Chemistry of Solids, 37, 619–624.

Muthukumarasamy, P., Nagarajan, T. and Narayanasamy, A. (1980) Mössbauer effect studies on $ZnCr_xFe_{2-x}O_4$. Journal of Physics, C, Solid State Physics 13, 3961–3968.

Navrotsky, A. and Kleppa, O. J. (1967) The thermodynamics of

cation distributions in simple spinels. Journal of Inorganic and Nuclear Chemistry, 29, 2701–2714.

Ok, H. N. and Evans, B. J. (1976) Collective electron description of the conductive mechanism in $M_xFe_{3-x}O_4$, M = Cd, Zn. Physical Review B, 14, 2956–2965.

Ok, H. N., Pan, L. S. and Evans, B. J. (1978) ^{57}Fe Mössbauer study of chromium doped magnetite $Fe_{3-x}Cr_xO_4$ ($O < x < 0.5$) above the Verwey transition. Physical Review B, 17, 85–90.

Olés, A. (1970) Neutron diffraction study of the $ZnFe_{(2-x)}Cr_{(x)}O_4$ series. Physica Status Solidi A, 569–577.

O'Neill, H. St C. and Navrotsky, A. (1984) Cation distributions and thermodynamic properties of binary spinel solid solutions. American Mineralogist, 69, 733–753.

O'Neill, H. St C. and Navrotsky, A. (1983) Simple spinels: crystallographic parameters, cation radii, lattice energies and cation distribution. American Mineralogist, 68, 181–194.

Petric, A. and Jacob, K. T. (1982) Thermodynamic properties of Fe_3O_4–FeV_2O_4 and Fe_3O_4–$FeCr_2O_4$ spinel solid solutions. Journal of the American Ceramic Society, 65, 117–123.

Popov, G. P. Simonova M. I. Ugol'nikova T. A. and Chufarov, G. I. (1963). Thermodynamic properties and crystallochemical characteristics of solid solutions of zinc ferrite with magnetite. Academy of Sciences of USSR Proceedings, Chemistry Section 148, 64–68.

Price, G. D., Price, S. L. and Burdett, J. K. (1982) The factors influencing cation site-preferences in spinels, a new Mendelyevian approach. Physics and Chemistry of Minerals, 8, 69–76.

Robbins, M., Wertheim, G. K., Sherwood, R. C. and Buchanan, D. N. E. (1971) Magnetic properties and site distributions in the system $FeCr_2O_4$–Fe_3O_4 ($Fe^{2+}Cr_{(2-x)}Fe^{3+}{}_{(x)}O_4$). Journal of the Physics and Chemistry of Solids, 32, 717–729.

Roeder, P. L., Campbell, I. H. and Jamieson, H. E. (1979). A re-evaluation of the olivine-spinel geothermometer. Contributions to Mineralogy and Petrology, 68, 325–334.

Sack, R. O. (1982) Spinels as petrogenetic indicators. Contributions to Mineralogy and Petrology, 79, 169–186.

Shannon, R. D. (1976) Revised effective ionic radii and systematic studies of interatomic distances in the halides and chalcogenides. Acta Crystallographica, A32, 751–767.

Srivastava, C. M. Shringi, S. N. and Srivastava, R. G. (1976) Mössbauer study of relaxation phenomena in zinc ferrous ferrites. Physical Review B, 14, 2041–2050.

Topsoe, H., Dumesic, J. A. and Boudait, M. (1974) Mössbauer spectra of stoichiometric and non-stoichiometric Fe_3O_4 microcrystals. Journal de Physica Colloque, C6, 411–414.

Trestman-Matts, A., Dorris, S. E., Kumarakrishnan, S. and Mason, T. O. (1983) Thermoelectric determination of cation distributions in Fe_3O_4–Fe_2TiO_4. The American Ceramic Society Journal (in press).

Urusov, V. S. (1983) Interactions of cations on octahedral and tetrahedral sites in simple spinels. Physics and Chemistry of Minerals, 9, 1–5.

Valentino, A. J. and Sclar, C. B. (1982) Experimental study of the magnetite ($FeFe_2O_4$)–franklinite ($ZnFe_2O_4$) solid solution series. (abstr.) EOS (Transactions of the American Geophysical Union) 63, 18, 470.

Verwey, E. J. W. and Heilmann, E. L. (1947) Physical properties and cation arrangement of oxides with spinel structures, The Journal of Chemical Physics, 15, 174–180.

Wu, C. C. and Mason, T. O. (1981) Thermopower measurement of cation distribution of magnetite. Journal of the American Ceramic Society, 64, 520–522.

Wu, C. C., Kumarakrishnan, S. and Mason, T. O. (1981) Thermopower composition dependence in ferrospinels. Journal of Solid State Chemistry, 37, 144–150.

Manuscript received, August 11, 1983;
accepted for publication, April 10, 1984.